

We are IntechOpen, the world's leading publisher of Open Access books Built by scientists, for scientists

5,800

Open access books available

142,000

International authors and editors

180M

Downloads

Our authors are among the

154

Countries delivered to

TOP 1%

most cited scientists

12.2%

Contributors from top 500 universities



WEB OF SCIENCE™

Selection of our books indexed in the Book Citation Index
in Web of Science™ Core Collection (BKCI)

Interested in publishing with us?
Contact book.department@intechopen.com

Numbers displayed above are based on latest data collected.
For more information visit www.intechopen.com



Wavelet Theory: Applications of the Wavelet

*Mohammed S. Mechee, Zahir M. Hussain
and Zahrah Ismael Salman*

Abstract

In this Chapter, continuous Haar wavelet functions base and spline base have been discussed. Haar wavelet approximations are used for solving of differential equations (DEs). The numerical solutions of ordinary differential equations (ODEs) and fractional differential equations (FrDEs) using Haar wavelet base and spline base have been discussed. Also, Haar wavelet base and collocation techniques are used to approximate the solution of Lane-Emden equation of fractional-order showing that the applicability and efficacy of Haar wavelet method. The numerical results have clearly shown the advantage and the efficiency of the techniques in terms of accuracy and computational time. Wavelet transform studied as a mathematical approach and the applications of wavelet transform in signal processing field have been discussed. The frequency content extracted by wavelet transform (WT) has been effectively used in revealing important features of 1D and 2D signals. This property proved very useful in speech and image recognition. Wavelet transform has been used for signal and image compression.

Keywords: Haar wavelet, continuous wavelet function, wavelet transform, B-cubic spline base

1. Introduction

Wavelets are special mathematical functions which have advantages over traditional Fourier methods in analyzing physical situations where the signal contains discontinuities and sharp spikes. The fields of applied mathematics such as quantum physics, seismic geology and electrical engineering have used and developed independently wavelets during last twenty years ago which leads to new wavelet applications such as image compression, radar, and earthquake prediction. Haar wavelet was initiated and independently developed by some authors. Wavelets can be summarized as a family of functions constructed from transformation and dilation of a single function called mother wavelet. From various types of continuous and discrete wavelets, Haar wavelet is the discrete type of wavelet which was first proposed and the first orthonormal wavelet basis is the Haar basis. Differential equations (DEs) are most important tools in mathematical models for physical phenomena. Many basis used to approximate the solutions of DEs. Haar wavelet is simple basis used to approximate the solution of DEs. [1] established a simple numerical method based on Haar wavelet operational matrix of integration for solving two dimensional elliptic partial differential equations (PDEs) of the form $\nabla^2 u(x,y) + ku(x,y) = f(x,y)$, [2]

used Haar wavelet operational matrix for the numerical solutions of FrDEs, [3] used Haar wavelet-quasi linearization technique for FrDEs, [4] used Haar wavelet method for solving FrPDEs numerically, [5] applied Haar wavelet transform to solve integral equations (IEs) and DEs, [6] solved 2D and 3D Poisson equations and biharmonic equations by the Haar wavelet method while [7] presented a numerical method for inversion of Laplace transform using the method of Haar wavelet operational matrix. The implementations of FrDEs which are used as mathematical models in many physically significant fields and applied science. Recently, the approximated solutions of the FrDEs have been studied using Haar wavelet method which shows to be more suitable to approximate the solutions of them. Nowadays, Haar wavelets are most widely and simplest due to their simplicity, the Haar wavelets are effective tools for approximating solutions of DEs. When this type of problem arises, mainly approximated solutions come to be available. From the many approximated methods, Haar wavelet approach is one to find the solutions of DEs. If the approximated solution gives less error than other methods, then, the method be an efficient method. However, one of interesting applications of wavelets bases is the approximation of DEs. Also, Haar wavelet technique is used to approximate the solutions of DEs of fractional-order. Wavelet transform is a mathematical approach widely used for signal processing applications. It can decompose special patterns hidden in mass of data. Wavelet transform has the advantage to simultaneously display functions and manifest their local characteristics in time-frequency domain. Wavelet transforms have had tremendous impact on the fields of signal processing, signal coding, estimation, pattern recognition, applied sciences, process systems engineering, econometrics, and medicine. Wavelet transforms are mainly divided into two groups; continuous wavelet transform (CWT) and discrete wavelet transform (DWT). The discretization of a voice transform generated by a representation of the Blaschke group on the Hardy space of the unit disk leads to the construction of analytic rational orthogonal wavelets. In this chapter, we introduce the concept of continuous wavelet functions together to the approximations solutions of DEs with ordinary- or fractional-order using Haar wavelet functions. Also, a comparison between Haar wavelet base with cubic spline base has been introduced. Wavelet transform as a mathematical approach has been discussed together to the applications of wavelet transform in signal.

1.1 Objectives of chapter

This chapter aims at achieving the following objectives:

1. To introduce continuous wavelet functions.
2. To use Haar wavelet approximations in solving of differential equations (DEs).
3. To imply Haar wavelet functions to approximate the solutions of DEs of fractional-order.
4. To compare Haar wavelet base with cubic spline base.
5. To study wavelet transform as a mathematical approach.
6. To discuss the discrete wavelet transform (DWT).
7. To study the applications of wavelet transform in signal processing field.

1.2 Scope of study

This chapter entailed the studying of continuous wavelet functions and Haar wavelet approximations. Wavelet transform introduced as a mathematical approach with some of applications of wavelet transform which is widely used in signal processing field. The approximation of DEs using Haar wavelet base was implemented with comparing to B-cubic spline base.

2. Preliminary

In this section, we introduce the definitions of two types of continues Haar wavelet functions and linear, quadratic and cubic spline functions base.

2.1 Continues Haar wavelet functions

Haar functions have been introduced by Hungarian mathematician. The orthogonal set of Haar functions is defined as a square waves with magnitude of ± 1 in some interval and zero elsewhere. The first curve is that $h_0(x) = 1$ during the whole interval $0 \leq x \leq 1$. The second curve $h_1(x)$ is the fundamental square wave, or mother wavelet which also spans the whole interval $[0, 1]$. All the other subsequent curve are generated from $h_1(x)$ with two operation translation and dilation. Haar wavelet functions defined as follows on $(0, X]$ [8].

$$h_0(x) = \frac{1}{\sqrt{M}} \quad 0 \leq x < X, \quad (1)$$

$$h_1(x) = \frac{1}{\sqrt{M}} \begin{cases} 1 & 0 \leq x < \frac{X}{2} \\ -1 & \frac{X}{2} \leq x < X \\ 0 & o.w. \end{cases} \quad (2)$$

$$h_i(x) = \frac{1}{\sqrt{M}} \begin{cases} \sqrt{2^j}, & \frac{k-1}{2^j}X \leq x < \frac{k-\frac{1}{2}}{2^j}X \\ -\sqrt{2^j}, & \frac{k-\frac{1}{2}}{2^j}X \leq x < \frac{k}{2^j}X \\ 0, & o.w. \end{cases} \quad (3)$$

for $i = 1, 2, 3, \dots, m-1$, $M = 2^j$ and $i = 2^j + k - 1$. We say that $h_1(x)$ is mother function and $h_i(x) = 2^{\frac{j}{2}}h_1(2^jx - k)$ for $i = 2, 3, \dots, m-1$. In general, we have the following: $h_0(x) = h_1\left(2^jx - \frac{k}{2^j}\right)$, where $n = 2^j + k, j \geq 0, 0 < k \leq 2^j$. Note that:

$$(h_p(x), h_q(x)) = \int_0^X h_p(x)h_q(x)dx = \frac{X}{m} \delta_{pq}.$$

To approximate $f(x)$ using Haar functions consider $f(x) = \sum_{i=0}^{m-1} a_i h_i(x)$. Then,

$$a_j = \frac{\int_0^X h_i(x)h_j(x)dx}{\int_0^X h_j^2(x)dx} = \frac{m}{X} \int_0^X f(x)h_j dx$$

for

$$j = 0, 1, 2, \dots, m - 1.$$

All Haar wavelets are orthogonal to each other:

$$\int_0^1 h_i(x)h_j dx = 2^{-j}\delta_{ij} = \begin{cases} 2^{-j}, & i = j = 2^{j+k} \\ 0, & i \neq j \end{cases}$$

2.2 Spline functions

The spline is used to refer to a wide class of smooth functions that are used in applications requiring data interpolation [9, 10]. The data may be either one-dimensional or multi-dimensional. Spline functions for interpolation are normally determined as the minimizers of suitable measures of roughness (for example integral squared curvature) subject to the interpolation constraints. Smoothing splines may be viewed as generalizations of interpolation splines where the functions are determined to minimize a weighted combination of the average squared approximation error over observed data and the roughness measure. For a number of meaningful definitions of the roughness measure, the spline functions are found to be finite dimensional in nature, which is the primary reason for their utility in computations and representation. For the rest of this section, the focus is entirely on one-dimensional, polynomial splines and the use of the term spline in this restricted sense. The base $\Phi(x) = \{\Phi_1(x), \Phi_2(x), \dots, \Phi_n(x)\}$ is called spline base of order n if the basis functions satisfy $\Phi_i(x) \in C^{n-1}(-\infty, \infty)$ for $i = 1, 2, \dots, n$. First of all, we partition $[0, 1]$ by choosing a positive integer n and defining $h = \frac{1}{n+1}$. This produces the equally-spaced nodes $x_i = ih$, for each $i = 0, 1, \dots, n + 1$. We then define the basis functions $\{\phi(x)\}_{i=0}^{n+1}$ on the interval $[0, 1]$.

2.2.1 Linear spline

The simplest spline is a piecewise polynomial function, with each polynomial having a single variable. The spline S takes values from an interval $[a, b]$ and maps them to \mathfrak{R} where $S : [a, b] \rightarrow \mathfrak{R}$. Since S is piecewise defined, choose k subintervals to partition $[a, b]$. The simplest choice of spline functions basis involves piecewise-linear polynomials. The first step is to form a partition of $[0, 1]$ by choosing points x_0, x_1, \dots, x_{n+1} . Letting $h_i = x_{i+1} - x_i$, for each $i = 0, 1, \dots, n$. We have defined the basis functions $\Phi_1(x), \Phi_2(x), \dots, \Phi_n(x)$. Linear spline is linear polynomial $S(x)$ which satisfies $S(x) \in C(-\infty, \infty)$. To construct linear spline base in which it can satisfy the boundary conditions $\phi_i(0) = \phi_i(1)$ for $i = 1, 2, \dots, n$. we have constructed the following component linear spline functions:

$$\Phi_i(x) = \begin{cases} 0, & 0 \leq x \leq x_{i-1}, \\ \frac{1}{h_{i-1}}(x - x_{i-1}), & x_{i-1} < x \leq x_i, \\ \frac{1}{h_i}(x_{i+1} - x), & x_i < x \leq x_{i+1}, \\ 0, & x_{i+1} < x \leq 1. \end{cases} \quad (4)$$

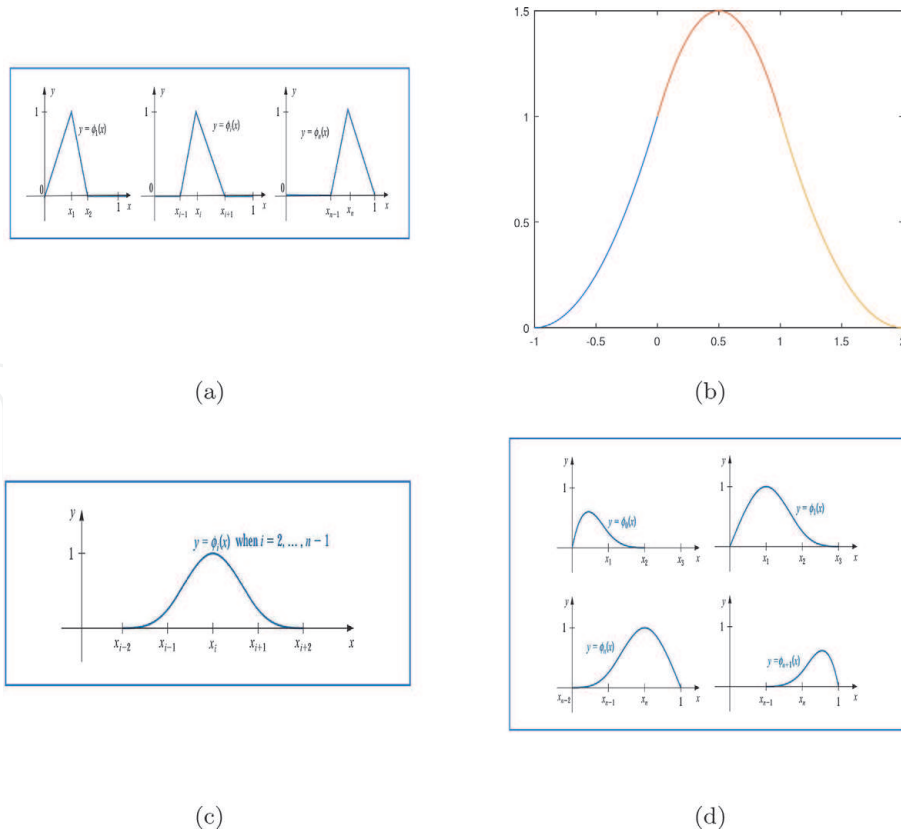


Figure 1.
 (a) Linear spline and (b) quadratic spline (c) cubic spline function and (d) compound cubic spline function.

for each $i = 1, 2, \dots, n$. (See **Figure 1(a)**, **Table 1(a)**). We can prove that the functions are orthogonal because $\Phi_i(x)$ and $\Phi_j(x)$ are nonzero only on (x_{i-1}, x_{i+1}) such that $\Phi_i(x)\Phi_j(x) = 0$ and $\Phi'_i(x)\Phi'_j(x) = 0$ if $i \neq j, j - 1, j + 1$, consequently, $\Phi_i(x) \in C(-\infty, \infty)$ for $i = 1, 2, 3, \dots, n$.

| x_i | $\Phi_i(x_i)$ | $\Phi'_i(x_i)$ | $\Phi''_i(x_i)$ |
|-----------|---------------|----------------|-----------------|
| x_{i-1} | 0 | | |
| x_i | 1 | | |
| x_{i+1} | 0 | | |
| (a) | | | |
| x_{i-1} | $\frac{1}{2}$ | 2 | |
| x_i | 1 | 0 | |
| x_{i+1} | $\frac{1}{2}$ | -2 | |
| (b) | | | |
| x_{i-2} | 0 | 0 | 0 |
| x_{i-1} | $\frac{1}{4}$ | $\frac{3}{4}$ | $-\frac{3}{2}$ |
| x_i | 1 | 0 | $-\frac{3}{4}$ |
| x_{i+1} | $\frac{1}{4}$ | $-\frac{3}{4}$ | $-\frac{3}{2}$ |
| x_{i+2} | 0 | 0 | 0 |
| (c) | | | |

Table 1.
 Values at node points (a) linear spline, (b) quadratic B-spline, and (c) cubic B-spline.

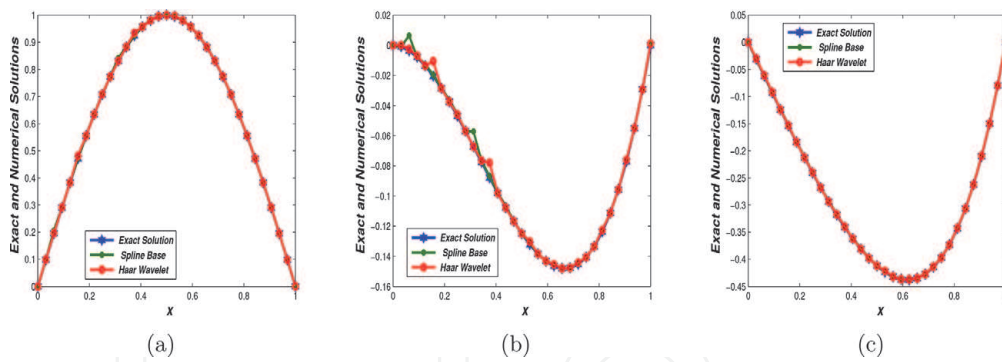


Figure 2. Comparison of Haar wavelet and Spline Base with exact solutions for examples (a) 3.5 (b) 3.6 (c) 3.7.

2.2.2 Quadratic B-spline

Quadratic B-spline is quadratic B-Spline polynomial $S(x)$ which satisfy $S(x) \in C^2(-\infty, \infty)$. To construct quadratic spline base in which satisfy the boundary conditions $\phi_i(0) = \phi_i(1)$ for $i = 1, 2, \dots, n$ we have constructed the following component quadratic spline functions (**Figure 2**):

$$\phi_i(x) = \frac{1}{h^2} \begin{cases} (x_{i+2} - x)^2 - 3(x_{i+1} - x)^2 + 3(x_i - x)^2; & [x_{i-1}; x_i]; \\ (x_{i+2} - x)^2 - 3(x_{i+1} - x)^2; & [x_i; x_{i+1}]; \\ (x_{i+2} - x)^2; & [x_{i+1}; x_{i+2}]; \\ 0; & o.w. \end{cases} \quad (5)$$

See **Figure 1(b)** and **Table 1(b)**.

2.2.3 Cubic B-spline

Many researchers used B-cubic spline base which defined as follows:

$$S(x) = \frac{1}{4} \begin{cases} 0, & x < -2 \\ (2+x)^3, & -2 \leq x \leq -1 \\ (2+x)^3 - 4(1+x)^3, & -1 < x \leq 0 \\ (2-x)^3 - 4(1-x)^3, & 0 < x \leq 1 \\ (2-x)^3, & 1 < x \leq 2 \\ 0, & x > 2. \end{cases} \quad (6)$$

Consequently, $S(x) \in C_0^2(-\infty, \infty)$.

To construct cubic spline base in which satisfy the boundary conditions $\phi_i(0) = \phi_i(1)$ for $i = 1, 2, \dots, n$ we have constructed the following component cubic spline functions:

$$\phi_i(x) = \begin{cases} S\left(\frac{x}{h}\right) - 4S\left(\frac{x+h}{h}\right), & i = 0 \\ S\left(\frac{x-h}{h}\right) - S\left(\frac{x+h}{h}\right), & i = 1 \\ S\left(\frac{x-ih}{h}\right), & 2 \leq i \leq n \\ S\left(\frac{x-nh}{h}\right) - S\left(\frac{x(n+2)h}{h}\right), & i = n \\ S\left(\frac{x-(n+1)h}{h}\right) - 4S\left(\frac{x-(n+2)h}{h}\right), & i = n+1. \end{cases} \quad (7)$$

See **Figure 1(c), (d)** and **Table 1(c)**.

3. Approximation of differential equations (DEs)

Mathematics has several tools to describe the problems in real life, engineering and science. ODEs and PDEs are significant tools in applied mathematics. They played significant rule in describing the mathematical models in applications of engineering, science and economics. High-order DE arises in some fields of engineering and science such as nonlinear optics and quantum mechanics. The approximated solutions of DEs should be studied when the ODEs and PDEs have no analytical solutions or it is very difficult to find the analytical solutions. The numerical or approximated solutions of DEs are very important in scientific computation, as they are widely used to model real life problems. In this section, we have studied the approximation solutions of DEs using spline and Haar wavelet bases (**Table 2**).

3.1 Approximation of ordinary differential equations (ODEs)

In this section, we have studied approximation solutions of ODEs using spline and Haar wavelet bases.

| $n \setminus t$ | 0 | 0.25 | 0.5 | 0.75 | 1 |
|-----------------|---|-----------|-----------|-----------|-----------|
| 5 | 0 | 1.3345e-3 | 0.0015 | 5.0673e-3 | 3.6339e-3 |
| | 0 | 1.311e-3 | 0.0005 | 5.0683e-3 | 3.6229e-3 |
| 10 | 0 | 1.3232e-5 | 2.6342e-5 | 1.5634e-6 | 4.1443e-5 |
| | 0 | 1.3211e-5 | 2.1212e-5 | 1.2341e-6 | 4.0101e-5 |
| 50 | 0 | 2.3416e-7 | 1.6611e-7 | 5.1126e-7 | 2.1233e-7 |
| | 0 | 2.1414e-7 | 1.2211e-7 | 5.2233e-7 | 2.1266e-7 |
| 100 | 0 | 4.9383e-8 | 3.4453e-8 | 5.0347e-8 | 6.4332e-7 |
| | 0 | 4.9121e-8 | 3.4564e-8 | 5.0111e-8 | 6.4222e-7 |

Table 2.

Absolute errors of example 3.1 using numerical collection method with (a) polynomial basis (b) Haar wavelet basis.

3.1.1 Approximation of DEs using spline functions

In this section, we have introduced the linear, quadratic and cubic B-spline base and their applications in solving ODEs. The operational matrices of the fractional-order integration of the B-spline base has been studied.

3.1.2 Rayleigh-Ritz Method

Rayleigh-Ritz method is variational technique for solving boundary value problems (BVPs) which is first reformulated as a problem of choosing, from set of all sufficiently differentiable functions satisfying the boundary conditions, the function to minimize a certain integral. To describe the Rayleigh-Ritz method, we consider the approximation of the solution to a linear of two-boundary value problem from beam-stress analysis. This BVP is described by the following DE:

$$-\frac{d}{dx} \left(p(x) \frac{dy}{dx} \right) + q(x)y(x) = f(x), \quad 0 \leq x \leq 1. \quad (8)$$

with boundary conditions

$$y(0) = y(1) = 0.$$

The DE describes the deflection $y(x)$ of a beam of length 1 with variable cross section represented by $q(x)$. The deflection is due to the added stresses $p(x)$ and $f(x)$. We have the following functional that is equivalent to Eq. (8).

$$I(u(x)) = \int_0^1 \left(p(x)(u'(x))^2 + q(x)(u(x))^2 - 2f(x)u(x) \right) dx. \quad (9)$$

An approximation

$$u(x) = \sum_{i=0}^n \Phi_i(x). \quad (10)$$

to the solution $y(x)$ of Eq. (9) can be obtained by finding the constants $c_1, c_2, c_3, \dots, c_n$ to minimize the integral Eq. (9): When considering $I(c_1, c_2, c_3, \dots, c_n)$ as a function of $c_1, c_2, c_3, \dots, c_n$ to have

$$\frac{\partial I}{\partial c_j} = 0$$

for $i = 1, 2, 3, \dots, n$.

Lastly, we have obtained the linear system of equations $Ac = b$, where,

$$a_{ij} = \int_0^1 \left(p(x)\Phi_i'(x)\Phi_j'(x) + q(x)\Phi_i(x)\Phi_j(x) \right) dx$$

and

$$b_i = \int_0^1 f(x)\Phi_i(x) dx,$$

for $i, j = 1, 2, \dots, n$ [10]. To implement the Ritz method we consider the following problems.

Example 3.1 [8]

Consider

$$y''(t) + y(t) = t^2 - t + 2, \quad 0 \leq t \leq 1, \quad (11)$$

subject to the initial condition is

$$y(0) = y(1) = 0,$$

with the exact solution $y(t) = t^2 - t$

Let $n = 5$, then,

$$a_{ij} = \int_0^1 \left(-h'_i(x)h'_j(x) + h_i(x)h_j(x) \right) dx = \frac{m}{X} \delta_{ij},$$

and

$$b_i = \int_0^1 (x^2 - x + 2)h_i(x)dx,$$

for $i, j = 1, 2, \dots, n$. However,

$$c = \left[-\frac{1}{3}, 0, \frac{1}{4\sqrt{2}}, -\frac{1}{4\sqrt{2}}, \frac{.0234375}{2} \right].$$

Example 3.2 [8].

Consider

$$y''(t) + \pi^2 y(t) = 0, \quad 0 \leq t \leq 1, \quad (12)$$

subject to the initial condition is

$$y(0) = y(1) = 0,$$

with the exact solution $y(t) = \sin \pi t$

Let $n = 10$, then,

$$a_{ij} = \int_0^1 \left(-h'_i(x)h'_j(x) + \pi^2 h_i(x)h_j(x) \right) dx = \pi^2 \frac{m}{X} \delta_{ij},$$

and

$$b_i = 0,$$

for $i, j = 1, 2, \dots, n$. However, $c = [1, 1, 2, 3, 1, 1, 1, 1, 1, 1]$.

3.1.3 Analysis of collection method

Let the differential operator L defined on the interval $I = [a, b]$. Define the collocation points $x_i = a + ih$ for $i = 0, 1, \dots, n$; where $h = \frac{b-a}{n}$ and n is the number of partitions on I . Discretize the functions

$$\Phi(x) = \{\Phi_1(x), \Phi_2(x), \Phi_3(x), \dots, \Phi_n(x)\}.$$

Suppose

$$y(x) = \sum_{i=1}^n c_i \Phi_i(x).$$

Put the approximation of $y(x)$ at the point x_j in the DE, we get the function coefficient matrix $\Phi_{ij} = \Phi_i(x_j)$ and $\Phi'_{ij} = \Phi'_i(x_j)$. The matrix of coefficients has the dimension $n \times n$. Any function $y(x)$ which is square integrable in the interval $(0, 1)$ can be expressed as an infinite sum of Haar wavelet. The above series terminates at finite terms if $y(x)$ is piecewise constant or can be approximated as piecewise constant during each subinterval.

3.2 The quadratic B-Spline Base

Consider the quadratic B-spline Base

$$S(x) = \{S_1(x), S_2(x), S_3(x), \dots, S_n(x)\}.$$

Suppose $y(x) = \sum_{i=1}^n c_i S_i(x)$. The general ODE of first-order has the following form

$$a_0(t)y'(t) + a_1(t)y(t) = f(t), \quad 0 \leq t \leq 1, \quad (13)$$

subject to the initial condition is $y(0) = \alpha$.

Example 3.3 [8].

$$y'(t) + y(t) = \sin(t) + \cos(t), \quad 0 \leq t \leq 1, \quad (14)$$

subject to the initial condition is

$$y(0) = 0,$$

The coefficients are $a_0(t) = a_1(t) = 1$ and $f(t) = \sin(t) + \cos(t)$.

Consider the quadratic B-spline base, then, the matrix of coefficients has the following formula:

$$A_{ij} = S'_i(t_j) + S_i(t_j),$$

and

$$b_i = \sin(t_i) + \cos(t_i)$$

for $i, j = 1, 2, \dots, n$. By solving the system of coefficients $Ac = b$ we will obtain the coefficients of approximation.

3.3 Approximation of DEs using Haar wavelet Functions Base

We introduce the Haar wavelet technique for solving general linear first-order ODEs [11].

3.3.1 First-order linear ODEs

Consider the following general linear first-order ODE:

$$y'(t) + f(t)y(t) = g(t); 0 \leq t \leq a; f(t) \neq 0, \quad (15)$$

$$y(0) = \beta. \quad (16)$$

Substituting $t = ax$ in Eq. (15) which reduces to

$$y'(x) + af(x)y(x) = ag(x); 0 \leq x \leq 1; f(x) \neq 0, \quad (17)$$

$$y(0) = \beta. \quad (18)$$

We assume that

$$y'(x) = \sum_{i=1}^k c_i h_i(x), \quad (19)$$

where c_i 's for $i = 1, 2, \dots, k$ are Haar coefficients to be determined. Integrating Eq. (19) with respect to x , we get the following

$$y(x) = \beta + \sum_{i=1}^k c_i P_{1,i}(x). \quad (20)$$

Substituting Eqs. (19) and (20) in Eq. (17), we get the following system of equation:

$$\sum_{i=1}^k c_i h_i(x) + af(x) \sum_{i=1}^k c_i h_i(x) = ag(x). \quad (21)$$

Put $x = t_j$ for $j = 1, 2, \dots, n$. in Eq. (21), we get linear system in which the matrix of coefficients has the following formula:

$$A_{ij} = (1 + af(t_i))h_i(t_j)$$

and

$$b_i = ag(t_j),$$

for $i, j = 1, 2, \dots, n$. By solving the linear system of coefficients $Ac = b$, we obtain the coefficients of approximated solution.

3.4 Approximation of fractional differential equations (FrDEs)

In this section, we have studied approximation of DEs using spline and Haar wavelet bases.

3.4.1 Operational matrix of the fractional order integration of the B-Spline Base

In this section, we have evaluated the operational matrices of the fractional-order integration of the linear, quadratic and cubic B-spline Base.

3.4.2 Linear spline

This subsection examines the cubic linear spline operational matrix $FS\alpha$ of integration of the fractional order as follows:

$$J_{x_i}^\alpha(x) = \frac{1}{\Gamma(\alpha+2)} \begin{cases} 0, & 0 \leq x \leq x_{i-1}, \\ \frac{1}{h_{i-1}} x_{i-1}^{\alpha+1}, & x_{i-1} < x \leq x_i, \\ \frac{1}{h_{i-1}} x_{i-1}^{\alpha+1} + \frac{1}{h_i} (ah_i x_i^\alpha - x_i^{\alpha+1}), & x_i < x \leq x_{i+1}, \\ 0, & x_{i+1} < x \leq 1. \end{cases} \quad (22)$$

where $x_{i-1} = x - x_{i-1}, x_i = x - x_i$.

3.4.3 Quadratic B-spline

This subsection introduced the quadratic B-spline operational matrix $FS\alpha$ of integration of the fractional order as follows:

$$J_x^\alpha(x) = JJ * \frac{1}{\Gamma(\alpha+3)},$$

where

$$JJ = \begin{cases} 2(x-1)^{\alpha+2}; & x \in [1, 2]; \\ 2(x-1)^{\alpha+2} - 6(x-2)^{\alpha+2}; & x \in [2, 3]; \\ 2(x-1)^{\alpha+2} - 6(x-2)^{\alpha+2} + 6(x-3)^{\alpha+2}; & x \in [3, 4]; \\ 0; & o.w. \end{cases} \quad (23)$$

3.4.4 Cubic B-spline

This subsection introduced the cubic B-spline operational matrix $FS\alpha$ of integration of the fractional order as follows:

$$J_x^\alpha(x) = JJ * \frac{1}{\Gamma(\alpha+4)},$$

where

$$JJ = \begin{cases} 0, & x < -2 \\ \frac{3}{2} x^{\alpha+3}, & -2 \leq x \leq -1 \\ \frac{3}{2} x^{\alpha+3} - 6x_1^{\alpha+3}, & -1 < x \leq 0 \\ \frac{3}{2} x^{\alpha+3} - 6x_1^{\alpha+3} + 9x_2^{\alpha+3}; & 0 < x \leq 1 \\ \frac{3}{2} x^{\alpha+3} - 6x_1^{\alpha+3} + 9x_2^{\alpha+3} - 6x_3^{\alpha+3}; & 1 < x \leq 2 \\ 0, & x > 2, \end{cases} \quad (24)$$

where $x_i = x - i; i = 1, 2, 3$.

3.5 Numerical Solutions of fractional differential equations

3.5.1 Numerical solutions of fractional differential equations using Haar base

We will introduce the Haar wavelet technique for solving FrDEs.

Example 3.4 [8].

Consider the general fractional-order linear DE

$$y^\alpha(t) = A(t) + B(t)y(t) = C(t); 0 \leq t \leq a; n - 1 < \alpha < n, \quad (25)$$

subject to initial conditions $y_j(0) = a_j$ for $j = 0, 1, \dots, n - 1$. where $A(t), B(t)$ and $C(t)$ are given functions, are arbitrary constants and α is a parameter describing the order of the fractional derivative. The general response expression contains a parameter describing the order of the fractional derivative that can be varied to obtain various responses.

Substituting $t = ax$ in Eq. (25) which reduces to

$$y^\alpha(x) = aA(x) + aB(x)y(x) = C(t); \quad 0 \leq x \leq 1; \quad n - 1 < \alpha < n, \quad (26)$$

$$y_j(0) = a_j; j = 0, 1, \dots, n - 1. \quad (27)$$

We assume that

$$y^\alpha(x) = \sum_{i=1}^k c_i h_i(x). \quad (28)$$

If $\alpha = \frac{1}{2}$, integrating Eq. (28) once, we get

$$y(x) = a_0 + \sum_{i=1}^k c_i FH_{\frac{1}{2},i}(x). \quad (29)$$

Substituting Eqs. (28) and (29) in Eq. (26), we get

$$\sum_{i=1}^k c_i h_i(x) - aA(x) - aB(x) \left(a_0 + \sum_{i=1}^k c_i FH_{\frac{1}{2},i}(x) \right) = C(x), \quad (30)$$

If $\alpha = \frac{3}{2}$, integrating Eq. (26) twice, we get

$$y^{\frac{1}{2}}(x) = a_1 + \sum_{i=1}^k c_i FH_{\frac{3}{2},i}(x), \quad (31)$$

and

$$y(x) = a_0 + a_1 x + \sum_{i=1}^k c_i FH_{\frac{3}{2},i}(x). \quad (32)$$

Substituting Eqs. (28) and (37) in Eq. (26), we get

$$\sum_{i=1}^k c_i h_i(x) - aA(x) - aB(x) \left(a_0 + \sum_{i=1}^k c_i FH_{\frac{3}{2},i}(x) \right) = C(x). \quad (33)$$

Put $x = t_j$ for $j = 1, 2, \dots, n$. in Eq. (30) in case $\alpha = \frac{1}{2}$, or in Eq. (33) in case $\alpha = \frac{3}{2}$, we get the linear system in which the matrix of coefficients has the following formula:

$$A_{ij} = h_i(x)(t_j) + aB(t_j)FH_{\alpha,i}(t_j)$$

and

$$b_i = C(t_j) + aA(t_j) - aa_0B(t_j),$$

for $i, j = 1, 2, \dots, n$. By solving the linear system of coefficients $Ac = b$ we obtain the coefficients of approximated solution $y(t)$ of Eq. (26).

3.5.2 Numerical solutions of fractional differential equations using B-spline base

We will introduce the B-spline technique for solving FrDE (26). Consider the quadratic B-spline base

$$S(x) = \{S_1(x), S_2(x), S_3(x), \dots, S_n(x)\},$$

Suppose

$$y(x) = \sum_{i=1}^n c_i S_i(x).$$

We assume that

$$y^\alpha(x) = \sum_{i=1}^k c_i S_i(x). \quad (34)$$

If $\alpha = \frac{1}{2}$, integrating Eq. (34) once, we get

$$y(x) = a_0 + \sum_{i=1}^k c_i FS_{\frac{1}{2},i}(x). \quad (35)$$

Substituting Eqs. (34) and (35) in Eq. (26), we get

$$\sum_{i=1}^k c_i S_i(x) - aA(x) - aB(x) \left(a_0 + \sum_{i=1}^k c_i FS_{\frac{1}{2},i}(x) \right) = C(x). \quad (36)$$

If $\alpha = \frac{3}{2}$, integrating Eq. (34) once, we get

$$y(x) = a_0 + a_1 x + \sum_{i=1}^k c_i FH_{\frac{3}{2},i}(x). \quad (37)$$

Substituting Eqs. (28) and (29) in Eq. (26), we get

$$y^{\frac{1}{2}}(x) = a_1 + \sum_{i=1}^k c_i FH_{\frac{1}{2},i}(x), \quad (38)$$

and

$$y(x) = a_0 + a_1 x + \sum_{i=1}^k c_i FH_{\frac{3}{2},i}(x), \quad (39)$$

$$\sum_{i=1}^k c_i S_i(x) - aA(x) - aB(x) \left(a_0 + \sum_{i=1}^k c_i FS_{\frac{3}{2},i}(x) \right) = C(x). \quad (40)$$

Put $x = t_j$ for $j = 1, 2, \dots, n$. in Eq. (36) in case $\alpha = \frac{1}{2}$, or Eq. (40) in case $\alpha = \frac{3}{2}$, we get the linear system in which the matrix of coefficients has the following formula:

$$A_{ij} = (h_i(x)(t_j)) + aB(t_j)FH_{\alpha,i}(t_j)$$

and

$$b_i = C(t_j) + aA(t_j) - aa_0B(t_j),$$

for $i, j = 1, 2, \dots, n$. By solving the linear system of coefficients, we obtain the coefficients of approximated solution $y(t)$ of Eq. (26).

3.5.3 Numerical solution of fractional Lane differential equation

We generalize the definition of Lane-Emden equations up to fractional order as following:

$$D^\alpha y(t) + \frac{k}{t^{\alpha-\beta}} D^\beta y(t) + f(t, y) = g(t); 0 < t \leq 1, k > 0, \quad (41)$$

with the initial condition $y(0) = A; y'(0) = B$ where $1 < \alpha \leq 2, 0 < \beta \leq 1$ and A, B are constants and $f(t, y)$ is a continuous real-valued function and $g(t, y) \in [0, 1]$. The theory of singular boundary value problems has become an important area of investigation in the past three decades. One of the equations describing this type is the Lane-Emden equation. Lane-Emden type equations, first published by [12], and further explored in detail by [13], represents such phenomena and having significant applications, is a second-order ODE with an arbitrary index, known as the polytropic index, involved in one of its terms. The Lane-Emden equation describes a variety of phenomena in physics and astrophysics. [14] imposed the Lane-Emden DE of fractional order and the approximate solution is obtained by employing the method of power series and a numerical solution is established by the least squares method for these Eqs. [14] approximate the solution of DE by employing the method of power series and the numerical solution is established by collection method.

3.5.3.1 Analysis of numerical method of fractional Lane differential equation

[15] studied the solution of DEs based on Haar operational matrix, [16] studied the solution of DEs using Haar wavelet collocation method, [17] studied the numerical solution of DEs by using Haar wavelets, [18] used Haar wavelet approach to ODEs, [19] solved the fractional Riccati DEs using Haar wavelet while [14] studied the fractional DEs of Lane-Emden type numerically by method of collocation. [20] introduced an operational Haar wavelet method for solving fractional Volterra integral equations, [21] solved fractional integral equations by the Haar wavelet method, [22] used Haar wavelet-quasi linearization technique for fractional nonlinear DEs, [21] solved the fractional integral equations by the Haar wavelet method, [4] used Haar wavelet method for solving fractional PDEs numerically. In Eq. (41), consider $\alpha > \beta, f(t, y) = \frac{1}{t^{\alpha+2}} y(t)$ and $g(t) = 0, .$

However, $D^\alpha W(t) = ah(t) = \sum_{i=0}^m c_i h_i(t)$ and

$$\begin{aligned} D^\beta W(t) &= (I^{\alpha-\beta} D^\alpha) W(t) + W^\beta(0) \\ &= ap^{\alpha-\beta} h(t) + W^\beta(0) \\ W(t) &= (I^\alpha D^\alpha) W(t) + W(0) \\ &= ap^\alpha h(t) + A. \end{aligned}$$

Hence,

$$ah(t) + \frac{k}{t^{\alpha-\beta}} ap^{\alpha-\beta} h(t) + W^\beta(0) + ap^\alpha h(t) + A = Ch(t).$$

If we consider $\alpha = \frac{3}{2}$ and $\beta = \frac{1}{2}$ we solve the system of equations to obtain the coefficients $(c_0, c_1, c_2, \dots, c_m)$.

3.6 Comparison study using numerical collection method

Collocation method for solving DEs is one of the most powerful approximated methods. This method has its basis upon approximate the solution of FrDEs by a series of complete sequence of functions, a sequence of linearly independent functions which has no non-zero function perpendicular to this sequence of functions. In general, $y(t)$ is approximated by [14].

$$y(t) = \sum_{i=1}^n a_i \Theta_i(t), \quad (42)$$

where a_i for $i = 1, 2, \dots, n$ are an arbitrary constants to be evaluated and Θ_i for $i = 1, 2, \dots, n$ are given set of functions. Therefore, the problem in Eq. (41) of evaluating $y(t)$ is approximated by (42) then, is reduced to the problem of evaluating the coefficients for $i = 0, 1, 2, \dots, n$.

Let $\{t_1, t_2, \dots, t_n\}$ is a partition to interval $[0, 1]$ and $t_j = jh$ and $h = \frac{1}{n}$ and $j = 0, 1, 2, \dots, n$. See the comparison of absolute errors of the problem using numerical collection method with polynomial basis and Haar wavelet basis.

Example 3.5 [8]

Consider

$$w''(t) + \pi^2 w(t) = 0, \quad (43)$$

with the boundary conditions

$$w(0) = w(1) = 0.$$

The exact solution is $w(t) = \sin \pi t$.

Example 3.6 [8]

Consider

$$t^2 w''(t) - 6w(t) = 4t^2, \quad (44)$$

with the boundary conditions

$$w(0) = w(1) = 0.$$

The exact solution is $w(t) = t^2(t - 1)$.

Example 3.7 [8]

Consider

$$w''(t) = w(t) + 4te^t, \quad (45)$$

with the boundary conditions

$$w(0) = w(1) = 0.$$

The exact solution is $w(t) = t(t - 1)e^t$.

4. Wavelet transform (WT)

Fourier transform (FT) of a time signal $x(t)$ reveals the frequency content of the signal by decomposing the signal using complex sinusoids as follows:

$$X(f) = F\{x(t)\} = \int_{-\infty}^{\infty} x(t)e^{-j2\pi ft} dt.$$

However, FT cannot reveal the time information associated with a specific frequency. This drawback enhanced research in the time-frequency domain [23]. One of the most important time-frequency distributions (TFD's) is the wavelet transform (WT), which is a time-frequency representation of signals. While not all TFD's are invertible, a big advantage of WT over many other TFD's is invertibility. WT proved to be successful in revealing spectral features of signals. Instead of sustainable waves like sinusoidal waves as in the case of Fourier transform, WT is based on decomposing signals using decaying waves (small waves, or wavelets), all are shifted and dilated versions of a specific wavelet called mother wavelet. The continuous wavelet transform (CWT) of a signal $x(t)$ using a mother wavelet $\psi(t)$ is given by:

$$W_x^\psi(t, s) = \frac{1}{\sqrt{s}} \int_{-\infty}^{\infty} x(\lambda) \cdot \psi^* \left(\frac{\lambda - t}{s} \right) d\lambda,$$

where λ is a representation of time inside the convolution integral, ψ^* is the complex conjugate of the wavelet ψ , and $s \in \mathfrak{R}^+ = \mathfrak{R} - \{0\}$ is called the "scale", which we expect to be inversely related to the radian frequency $\omega = 2\pi f$ for the above structure to be comparable to the structure of the sinusoidal waves $\sin \omega(t)$ used in the Fourier transform; the actual scale-frequency relationship is given by:

$$s \approx \frac{K}{f}$$

where $K = f_m \cdot f_s$; $f_m = \arg(\max \{\psi(f)\})$; $\psi(f) = F\{\psi(t)\}$; f_s is the sampling frequency used to discretize $\psi(t)$ while computing $\psi(f)$ via DFT. It is apparent that, for a fixed scale s , the wavelet transform $W_x^\psi(t, s)$ is given by the convolution between the signal and the time-reversed wavelet as follows:

$$W_x^\psi(t, s) = x(t) \odot h(t)$$

where

$$h(t) = \left[\frac{1}{\sqrt{s}} \psi^* \left(\frac{-t}{s} \right) \right]$$

and \odot refers to the 1D convolution process:

$$x(t) \odot h(t) = \int_{-\infty}^{\infty} x(\lambda)h(t - \lambda)d\lambda$$

This fact gives another equivalent expression for $W_x^\psi(t, s)$ using Fourier transforms of the signal and the wavelet as follows:

$$W_x^\psi(t, s) = F^{-1}\{X(f).H(f)\} = \int_{-\infty}^{\infty} X(f).H(f)e^{+j2\pi ft}df$$

where $H(f) = F\{h(t)\}$. Hence, $W_x^\psi(t, s)$ can be implemented via filtering the signal $x(t)$ by a filter whose impulse response is $h(t)$. This will be the basis for implementing the discrete 1D and 2D wavelet transforms as explained below.

Generally speaking, Fourier transform $X(f) = F\{x(t)\}$ decomposes the signal $x(t)$ using the same sinusoidal wave $e^{-j2\pi ft}$ at different values of frequency f , while the wavelet transform $W_x^\psi(t, s)$ decomposes the signal $x(t)$ using the same mother wavelet $\psi(t)$ at different values of scale s (hence, frequency, f) and time t ; where both time and frequency information are revealed.

The WT is invertible, giving it a great advantage in applications:

$$x(t) = \frac{1}{c_\psi} \int_{-\infty}^{\infty} \int_{-\infty}^{\infty} W_x^\psi(\lambda, s) \cdot \frac{1}{s^2} \psi\left(\frac{t - \lambda}{s}\right) d\lambda ds$$

where $c_\psi = \int_{-\infty}^{\infty} \frac{|\psi(f)|}{|f|} df$, which implies that $\psi(0) = 0 \rightarrow \int_{-\infty}^{\infty} \psi(t)dt = 0$, hence, $\psi(t)$ must be oscillating. Also, to satisfy Parseval's Theorem we should have $\int_{-\infty}^{\infty} \psi(t)dt = 1$. The above continuous wavelet transform can be discretized to give the discrete wavelet transform (DWT), which can be implemented (as 1D DWT) by passing the signal $x(t)$ through a low-pass filter followed by down-sampling with a factor of 2 (giving approximation coefficients), and a high-pass filter then down-sampling by a factor of 2 (giving detail coefficients). These filters differ according to the analyzing wavelet [24]. The 2D DWT (for images) can be designed based on 1D DWT via tensor products, and it results into a decomposition of approximation coefficients at level k into four components: low-pass component that contains the approximation coefficients at level $k + 1$, and three high-pass components that contain the detail coefficients in three directions (horizontal, vertical, and diagonal). Note that approximation at level $k = 0$ is equivalent to the original 2D signal [24].

4.1 Some applications of the wavelet transform

The frequency content extracted by wavelet transform (WT) has been effectively used in revealing important features of 1D and 2D signals. This property proved very useful in speech and image recognition [25]. Also, the orthogonality of WT paved the way for using WT in orthogonal frequency division multiplexing (OFDM), a pivotal technique for 4th and 5th generations of digital communication [26]. In addition to that, WT proved to put high focus on the low-frequency part of the signal, in which most of the information resides, hence, WT has been used for signal and image compression [27]. The compression process can be performed using hard-thresholding of the WT as follows:

$$t(x) = \begin{cases} x & |x| \geq T \\ 0 & |x| < T \end{cases} \quad (46)$$

where $t(x)$ is the new WT coefficient value to replace the original coefficient x , and T is the threshold. Better compression results (in terms of signal size) can be obtained by increasing the threshold, however, larger deviation from the original signal (i.e., larger error) is obtained. Hence, choice of the threshold involves a trade-off between size and error. Original signal can be obtained from the compressed one via inverting the thresholded WT.

4.2 Noise removal using WT

An important application of the Wavelet Transform is noise removal from signals and images. As most of the information content of real-life signals is in the low-frequency regions, removal of high frequency regions in the WT of signals can help in removing the majority of noise. This can be done via thresholding WT coefficients or by removing the details coefficients of WT and considering only the approximation coefficients of WT. This property of separating low-frequency content from high-frequency content in the WT is mainly due to the filtering involved in the structure of WT as explained above. Noise removal using WT is more efficient for 1D signals corrupted by 1D noise process, where the 2D structure of WT in joint time-frequency domain can spread the 1D noise effect into a 2D plane, hence the noise power is greatly reduced. For noise removal, a soft-threshold can be used to cut out high-frequency coefficients as follows:

$$t(x) = \begin{cases} \text{sign}(x)(|x|-T) & |x| \geq T \\ 0 & |x| < T \end{cases} \quad (47)$$

where $t(x)$ is the new WT coefficient value to replace the original coefficient x , T is the threshold, and $\text{sign}(x)$ is the signum function defined as follows:

$$\text{sign}(x) = \begin{cases} +1 & x > 0 \\ 0 & x = 0 \\ -1 & x < 0 \end{cases} \quad (48)$$

Figure 3 shows the use of WT to denoise an image, while **Figure 4** shows the denoising of 1D signal using WT, where WT is performed on MATLAB via the wavelet Daubechies 3,

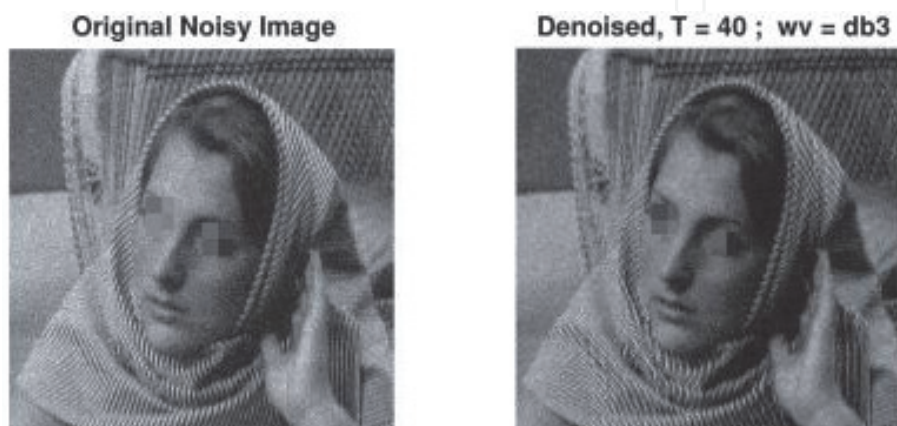


Figure 3.
 Image denoising using WT with soft threshold.

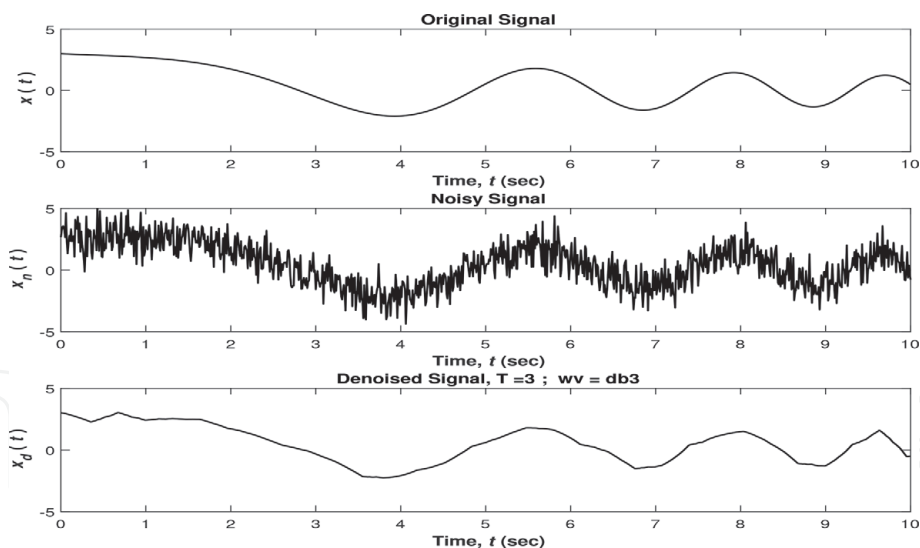


Figure 4.
1D signal denoising using WT with a hard threshold.

5. Discussion and conclusion

The numerical solutions of differential equations using Haar wavelet technique have been studied. Haar wavelet technique is used to approximate the solutions of DEs. The results which obtained form numerical solutions of ordinary differential equations as well as fractional differential equations by Haar collection method are compared with spline base. The numerical results have clearly shown the advantage and the efficiency of the techniques in terms of accuracy and computational time. Special initial value problem of Lane-Emden equation has been solved to show the applicability and efficacy of the Haar wavelet method. Wavelet transform as a mathematical approach has been studied and the applications of wavelet transform in signal processing field have been introduced. The wavelet transform has been effectively used to reveal on the features signals and the compression of signal and image.

Author details


Mohammed S. Mechee^{1*}, Zahir M. Hussain¹ and Zahrah Ismael Salman²

¹ University of Kufa, Najaf, Iraq

² Department of Mathematics, Faculty of Basic Education, Misan University, Amarah, Iraq

*Address all correspondence to: mohammeds.abed@uokufa.edu.iq

IntechOpen

© 2020 The Author(s). Licensee IntechOpen. This chapter is distributed under the terms of the Creative Commons Attribution License (<http://creativecommons.org/licenses/by/3.0>), which permits unrestricted use, distribution, and reproduction in any medium, provided the original work is properly cited. 

References

- [1] N. A. Ghani, "Numerical solution of elliptic partial differential equations by haar wavelet operational matrix method," *Thesis, university Malaya*, 2012.
- [2] F. A. Shah and R. Abbas, "Haar wavelet operational matrix method for the numerical solution of fractional order differential equations," *Nonlinear Engineering*, vol. 4, no. 4, pp. 203–213, 2015.
- [3] U. Saeed and M. ur Rehman, "Haar wavelet–quasilinearization technique for fractional nonlinear differential equations," *Applied Mathematics and Computation*, vol. 220, pp. 630–648, 2013.
- [4] L. Wang, Y. Ma, and Z. Meng, "Haar wavelet method for solving fractional partial differential equations numerically," *Applied Mathematics and Computation*, vol. 227, pp. 66–76, 2014.
- [5] Ü. Lepik, "Application of the haar wavelet transform to solving integral and differential equations," in *Proceedings of the Estonian Academy of Sciences, Physics, Mathematics*, vol. 56, no. 1, 2007.
- [6] Z. Shi and Y. Cao, "Application of haar wavelet method to eigenvalue problems of high order differential equations," *Applied Mathematical Modelling*, vol. 36, no. 9, pp. 4020–4026, 2012.
- [7] S. M. Aznam, "A study of the hyperbolic heat conduction problem and laplace inversion using generalized haar wavelet operational matrix method," *Thesis, university Malaya*, 2012.
- [8] O. I. A.-S. . M. S. Mechee, "A study of haar wallet for solving differential equations with some applications," *Thesis, university of Kufa*, 2018.
- [9] M. S. Mechee, "Numerical and approximated solutions of partial differential equations," *Thesis, university of Bagdad*, 1991.
- [10] D. Faires and Burden, *Numerical Methods*. Thomson Learning, 2003.
- [11] M. S. Mechee, O. I. Al-Shaher, and G. A. Al-Juaifri, "Haar wavelet technique for solving fractional differential equations with an application," in *AIP Conference Proceedings*, vol. 2086, no. 1. AIP Publishing LLC, 2019, p. 030025.
- [12] J. Homer Lane, "On the theoretical temperature of the sun under the hypothesis of a gaseous mass maintaining its volume by internal heat and depending on the laws of gases known to terrestrial experiment," *Am. J. Sci., 2d Ser*, vol. 50, pp. 57–74, 1870.
- [13] R. Emden, "Gaskugeln, bg teubner, leipzig and berlin," *Google Scholar*, p. 448, 1907.
- [14] M. Mechee and N. Senu, "Numerical study of fractional differential equations of lane-emden type by method of collocation," *Applied Mathematics*, vol. 3, no. 08, pp. 851–856, 2012.
- [15] N. Berwal, D. Panchal, and C. Parihar, "Solution of differential equations based on haar operational matrix," *Palestine journal of mathematics*, vol. 3, no. 2, pp. 281–288, 2014.
- [16] B. Sahoo, "A study on solution of differential equations using haar wavelet collocation method," Ph.D. dissertation, 2012.
- [17] Z. Shi, L.-Y. Deng, and Q.-J. Chen, "Numerical solution of differential equations by using haar wavelets," in *Wavelet Analysis and Pattern Recognition, 2007. ICWAPR'07. International*

Conference on, vol. 3. IEEE, 2007, pp. 1039–1044.

[18] R. Chen, “Haar wavelet approach to ordinary differential equation,” Ph.D. dissertation, California State Polytechnic University, Pomona, 2016.

[19] Y.-l. Li and L. Hu, “Solving fractional riccati differential equations using haar wavelet,” in *Information and Computing (ICIC), 2010 Third International Conference on*, vol. 1. IEEE, 2010, pp. 314–317.

[20] H. Saeedi, N. Mollahasani, M. M. Moghadam, and G. N. Chuev, “An operational haar wavelet method for solving fractional volterra integral equations,” *International Journal of Applied Mathematics and Computer Science*, vol. 21, no. 3, pp. 535–547, 2011.

[21] Ü. Lepik, “Solving fractional integral equations by the haar wavelet method,” *Applied Mathematics and Computation*, vol. 214, no. 2, pp. 468–478, 2009.

[22] U. Saeed and M. Rehman, “Haar wavelet picard method for fractional nonlinear partial differential equations,” *Applied Mathematics and Computation*, vol. 264, pp. 310–322, 2015.

[23] Z. M. Hussain and B. Boashash, “Design of time-frequency distributions for amplitude and if estimation of multicomponent signals,” in *Proceedings of the Sixth International Symposium on Signal Processing and its Applications (Cat. No. 01EX467)*, vol. 1. IEEE, 2001, pp. 339–342.

[24] Y. Meyer and D. H. Salinger, “Wavelets and operators,” 1995.

[25] M. P. Sampat, Z. Wang, S. Gupta, A. C. Bovik, and M. K. Markey, “Complex wavelet structural similarity: A new image similarity index,” *IEEE transactions on image processing*, vol. 18, no. 11, pp. 2385–2401, 2009.

[26] K. Abdullah, A. Z. Sadik, and Z. M. Hussain, “On the dwt-and wpt-ofdm versus fft-ofdm,” in *2009 5th IEEE GCC Conference & Exhibition*. IEEE, 2009, pp. 1–5.

[27] N. Al-Hinai, K. Neville, A. Z. Sadik, and Z. M. Hussain, “Compressed image transmission over fft-ofdm: A comparative study,” in *2007 Australasian Telecommunication Networks and Applications Conference*. IEEE, 2007, pp. 465–469.